



Executive summary

A Statistical Outlier Detection Method of EGNOS Integrity Performance Data

Problem area

The actual development of satellite navigation systems is crucial and includes after the introduction of EGNOS (augmentation of GPS), the planned modernization of GPS, and the new designed Ueropean Galileo system. For safety of life applications of satellite navigation systems, in e.g. aviation, reliability in the sense of integrity, availability and continuity is essential. In order to test the integrity, availability and continuity, a test methodology is required. This methodology should meet the requirement to be able to perform the analysis based on a limited amount of data collected within an acceptable observation time. This report presents a test method for analyzing the integrity of receiver output data possibly contaminated with outliers.

Description of work

A practical method to analyze the receiver integrity output data has been developed. As a test case the method has been applied to data

gathered during a test campaign of limited duration for EGNOS. With this method an accurate estimate of the integrity can be made. The applied theory including the outlier detection is presented.

Results and conclusions

From the test case presented in this report, it can be concluded that the estimation of the integrity on the basis of a limited number of test campaign data is possible indeed. The results of the test case show that the integrity did satisfy the requirements. These results also show that outliers occur indeed and must be taken into account in order to assess the integrity performance correctly.

Applicability

The software being developed is to be used to analyze measurement data gathered during test campaigns for SBAS and the future Galileo satellite navigation system.

Report no.

NLR-TP-2008-139

Author(s)

H. Kannemans

Report classification

UNCLASSIFIED

Date

May 2008

Knowledge area(s)

Methods for Development and Qualification of Avionics

Descriptor(s)SBAS
EGNOS
GNSS

A Statistical Outlier Detection Method of EGNOS Integrity Performance Data

Nationaal Lucht- en Ruimtevaartlaboratorium, National Aerospace Laboratory NLR

Anthony Fokkerweg 2, 1059 CM Amsterdam,
P.O. Box 90502, 1006 BM Amsterdam, The Netherlands

Telephone +31 20 511 31 13, Fax +31 20 511 32 10, Web site: www.nlr.nl



NLR-TP-2008-139

A Statistical Outlier Detection Method of EGNOS Integrity Performance Data

H. Kannemans

This report is based on a presentation held at the Institute of Navigation National Technical Meeting 2008, San Diego (U.S.A.), January 28-30, 2008.

The contents of this report may be cited on condition that full credit is given to NLR and the author.

This publication has been refereed by the Advisory Committee AEROSPACE SYSTEMS & APPLICATIONS.

Customer	National Aerospace Laboratory NLR
Contract number	----
Owner	National Aerospace Laboratory NLR
Division NLR	Aerospace Systems & Applications
Distribution	Unlimited
Classification of title	Unclassified
	May 2008

Approved by:

Author	Reviewer	Managing department
HK 22/5/08	JV 22/5/08	[Signature] 26/05/08



Summary

This report presents a practical method of analyzing the integrity of SBAS on the basis of test data gathered during a test campaign of limited duration. The method determines also possible outliers which turn out to be essential in order to obtain the correct integrity performance results. Dedicated software has been developed to demonstrate this test method. The applied theory is described and the results from test campaign data are analysed and discussed.



Contents

INTRODUCTION	4
THEORY	5
DISCUSSION OF TEST RESULTS OF THE NOVATEL MILLENNIUM RECEIVER	7
CONCLUSIONS	15
REFERENCES	15

A Statistical Outlier Detection Method of EGNOS Integrity Performance Data

H. Kannemans, *NLR – National Aerospace Laboratory, The Netherlands*

BIOGRAPHY

Henri Kannemans completed his study at the Technical University Delft in 1976. He works as a scientist at the Flight Test Systems department of the National Aerospace Laboratory – NLR. He is experienced in aircraft simulator model development and validation, wake vortex research for aircraft separation criteria, GNSS verification flight testing and he is currently involved in preparations for verification of the future Galileo program.

ABSTRACT

For safety of life applications of satellite navigation systems, in e.g. aviation, reliability in the sense of integrity, availability and continuity is essential. In order to test the integrity, availability and continuity, a test methodology is required. This methodology should meet the requirement to be able to perform the analysis based on a limited amount of data collected within an acceptable observation time. This paper presents a test method for analyzing the integrity of receiver output data possibly contaminated with outliers. In the paper the analysis of integrity is discussed in detail.

Usually one presents the test results in so-called Stanford diagrams visualizing the occurrence of Hazardous Misleading Information (HMI). Since the probability of HMI is very low, very often, no HMI condition occurs during the tests and in that case the computed HMI probability on this basis will then often be zero, being obviously incorrect. The method developed starts from the determination of two probability density functions: the fitted or measured probability density function of the protection level and the probability density function related to the position error, together forming a two dimensional probability density function.

A complicating factor in analyzing the probability density functions is the fact that due to the low probability of events occurring in the tail of the probability distributions this analysis is sensitive to outliers. So a method accounting for outliers must be incorporated in the method.

From the test case presented in this paper, it is concluded that the estimation of the integrity on the basis of a limited number of test campaign data is possible indeed. It also turns out that the analysis of outliers is absolutely necessary to obtain useful results. The results show that the integrity satisfied the ICAO requirement for the APV-I, APV-II and CAT-I aeronautical services during the actual test case.

INTRODUCTION

For safety of life applications of satellite navigation systems, in e.g. aviation, reliability in the sense of integrity, availability and continuity is essential. In order to test the performance with regard to these characteristics a test methodology is required. This methodology should meet the requirement to be able to perform the analysis based on a limited amount of data collected within an acceptable observation time. This paper describes a practical method of testing the integrity of SBAS on the basis of test data possibly contaminated with outliers. Matlab software has been developed to demonstrate this test methodology. For SBAS the protection level having a relationship with the position error is the basis for integrity (Ref. 1).

The GNSS integrity performance requirement for the ICAO navigation service levels APV-I, APV-II and CAT-I is 2×10^{-7} per approach. Assuming a duration of 150 seconds per approach it turns out that an integrity failure may occur once per 75×10^7 seconds or once per 23.8 years. Testing the EGNOS (European Geostationary Navigation Overlay Service) system by collecting data over 23.8 years is far from practical and still insufficient from a statistical point of view. So one needs to invent a way to do integrity tests on the basis of a limited amount of data to be collected within an acceptable observation time. The test method presented in this paper is based on the determination of the probability that an integrity failure may occur each independent measurement sample. Once this probability distribution is known the integrity risk can be computed.

The integrity tests for SBAS are to be based on the determined protection levels as a function of the position errors (the so-called Stanford diagrams, see for example Ref. 2 and 3). The method is meant to gain confidence

that the integrity requirement is met on the basis of a test campaign.

As a test case the method has been applied to data gathered during a test campaign of limited duration for EGNOS.

THEORY

The HMI (Hazardous Misleading Information) probability depends on two basic parameters: the actual position error and the determined protection level. Usually one presents the test results in the so-called Stanford diagrams visualizing the occurrence of Hazardous Misleading Information. In case the Protection Level is smaller than the Alarm Limit while the position error is larger than the Alarm Limit the position information is obviously misleading and is considered to be a Hazardous Misleading Information result. Since the probability of HMI is very low, it is not practical to state that the HMI probability is the ratio of the number of HMI results divided by the total number of measured samples. Very often, no HMI condition occurs during the tests. The resulting number of HMI conditions will then be zero and in that case the computed HMI probability on this basis will be zero as well, being obviously incorrect. Therefore, one needs to invent a correct way in obtaining a realistic estimate of the HMI probability also called the integrity risk. The method developed for this purpose starts from the determination of two probability density functions: the fitted or measured probability density function of the protection level and a probability density function related to the position error, together forming a two dimensional probability density function.

Once the position error is larger than the protection level we interpret that situation as misleading and accordingly it is called Misleading Information (MI).

It is well known that the vertical, north and east component of the position error do behave very similarly to the normal (Gaussian) probability density function. Since the horizontal position error is composed of two distributions, a normal distribution in north direction and a normal distribution in east direction, the horizontal position error must behave similarly to the Rayleigh probability density function.

A complicating factor in analyzing the probability density functions is the fact that due to the low probability of events occurring in the tail of the probability distributions this analysis is sensitive to outliers. So a detection method enabling the detection of outliers must be incorporated in the method. It turned out that outliers are present indeed influencing the estimated MI and HMI probabilities significantly.

Theory of outliers

Outliers are generally described as data points that do not seem to fit with the bulk of the data. In this paper, the data

is subdivided into a part related to typical system performance and a part related to atypical system performance, and the term outliers will be used for all data points that are (assumed to be) related to atypical performance. Typical performance is characterised by relatively small magnitude and high probability of occurrence whereas atypical performance is characterised by relatively large magnitude and (very) small probability of occurrence. In case the probability density of typical performance is modelled as a gaussian probability density, the outliers cause an increase in the total probability density relative to the normal density over the range of the outliers.

To allow visual inspection of the outliers it is useful to plot the probability density on a logarithmic scale (see figure 1). The measured (in this case simulated) outliers are clearly visible now

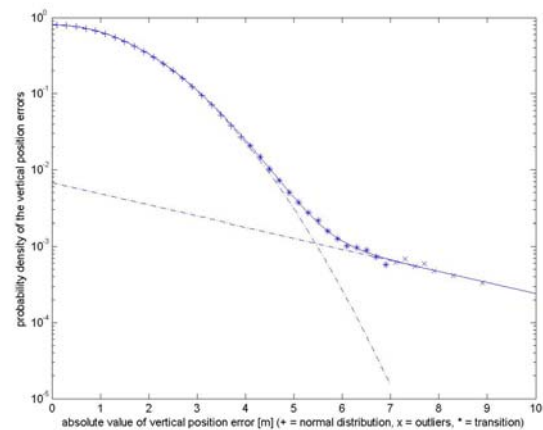


Figure 1: Example of outliers; symmetrical distribution with a mean value of zero (simulation).

In this paper it will be shown that an outlier probability distribution for EGNOS can be described by the Laplace distribution.

The equation for the Laplace probability density is:

$$f_{Laplace}(x | \mu, \lambda) = \frac{1}{2\lambda} \exp\left(-\frac{|x - \mu|}{\lambda}\right) \quad (1)$$

Here, μ is a location parameter and $\lambda > 0$ is a scale parameter.

The total probability density is the superposition of the normal probability density and the Laplace density:

$$f_{total_vertical} = (1 - \alpha) f_{Normal} + \alpha f_{Laplace} \quad (2)$$

where α is the fraction of outliers actually present in the probability density function.

In case of the vertical position error a symmetrical probability density function is assumed having a zero

mean. This assumption should be valid in case data are collected over a long period of time.

The outlier probability density can now very well be described as follows:

$$af_{Laplace} = \exp(a + b|x|) \quad (3)$$

Herein are a and b coefficients (parameters); a is the logarithmic Laplace density at $x = 0$ and b is the slope of the logarithmic Laplace density.

The horizontal probability density can be described with the following equation:

$$f_{total_{horizontal}} = (1 - \alpha)f_{Rayleigh} + \alpha r s f_{Laplace} \quad (4)$$

where $r = \sqrt{\text{north_error}^2 + \text{east_error}^2}$ is the horizontal position error and s is a scale parameter. Figure 2 shows this function.

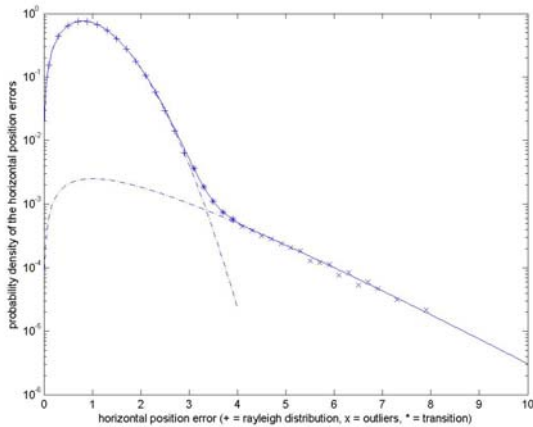


Figure 2: Example of outliers; Rayleigh distribution combined with Laplace distribution (simulation).

The point where the Laplace density takes over from the normal probability density is to be determined prior to setting up equation 2. This can be done by looking at the ratio between the measured probability density function and the normal probability density function (see figure 3). In practice a threshold of about 4 is right to distinguish the Laplace density from the combined density. A higher value (for example 10) is required to distinguish the Laplace density also from the transition region.

Knowing the region where the Laplace density is valid enables the estimation of the two parameters a and b in equation 3. These two parameters can very well be estimated by using linear regression.

After subtraction of the just estimated Laplace density from the measured probability density function, the normal probability density can be determined.

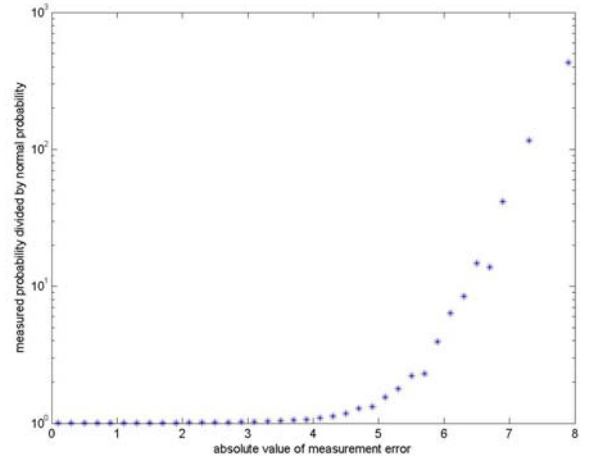


Figure 3: Example of outliers; measured probability divided by normal probability (simulation).

Confidence of the statistical results

It is good practice to determine an indication of the repeatability of final statistical results. This can be done by computing a so-called confidence interval.

For the normal probability distribution of a large amount of collected data the confidence interval is to be computed as follows:

$$\sigma_{confidenceInterval} = \sigma \sqrt{\frac{2}{n}} \quad (5)$$

where n is the number of independent observations. Due to the fact that the successive measured samples (1 Hz) are highly correlated, the number n is not equal to the number of observations. A better guess of this figure is $n=2$ (usually day and night behave differently, so we may assume $n=2$ is a minimum) for a test day of 24 hours. This may be too low; however one should keep in mind that the integrity risk is strongly affected by possible outliers and not by the normal probability distribution. Therefore it is not useful to study the value of the parameter n in equation 5 in much detail. So it is anyway required to compute the confidence interval of the Laplace density. This is possible using the regression analysis software already in use to estimate the Laplace density according to equation 3. The underlying theory of regression can be found in many text books.

Dependency of σ_{XPE} on XPL

Since the uncertainty in the position error increases with the computed protection level we need to estimate the probability density function in slices (bins) as a function of the protection level. From a theoretical point of view the standard deviation of the position error vary with the

protection level in a linear way and may even vary exactly in ratio with the protection level.

Thus the following relationship holds:

$$\sigma_{XPE_{measured}} = \sigma_0 + XPL * const_{XPL} \quad (6)$$

where XPL stands for VPL or HPL.

In this equation σ_0 could theoretically be zero, however, from many observations it follows that σ_0 is definitely positive. Furthermore the coefficient $const_{XPL}$ is always positive as well (see for example the figures 14 and 25). It must be noted here that equation 6 is to be estimated using a weighed least squares method where the weighing function is identical to the amount of measurement samples within each slice as a function of the XPL.

Simplification of the two dimensional probability distribution

In the paper it will be shown that the coefficients a and b in the Laplace density described by equation 3 often vary almost randomly as a function of XPL (see for example the figures 12 and 13). Consequently it makes sense to replace the Laplace distribution for each slice as a function of XPL by one common Laplace distribution. This implies that all measurement data are be mapped onto one common reference XPL. As reference XPL we choose a value of $XPL_{ref} = 10$ m, which is an arbitrary choice in essence. The mapping function used here is described by equation 6. Especially this mapping function makes sense since in that case the normal probability density as well as the Rayleigh density function is already treated in a common way. As an additional result the outliers are now uniformly treated, according to equation 6, in a common way too.

MI and HMI probability computation

To compute the MI and HMI probabilities, the following computational steps must be undertaken:

- The standard deviation of the normal distribution (vertical) or Rayleigh distribution (horizontal) together with the Laplace outlier distribution valid for $XPL_{ref} = 10$ m (this 10 m is chosen arbitrarily) are determined as described in the previous subchapters.
- From the parameters determined in the previous step, the probability distribution is evaluated over the range $XPE = 0$ through 200 m at $XPL_{ref} = 10$ m, where XPE stands for VPE or HPE.
- Using equation 6 the probability distribution at $XPL_{ref} = 10$ m is mapped over the area within the range $XPL = 0$ through 100 m in slices of 0.2 m. Each slice is weighed with the number of observations collected in that slice. At this stage

the 2 dimensional probability density function is known.

- The MI probability is computed by integration of the 2 dimensional probability density function over the area where $XPE > XPL$.
- The HMI probability is computed by integration of the 2 dimensional probability density function over the area where $XPE > XAL$ and $XPL < XAL$, where XAL stands for VAL or HAL.

DISCUSSION OF TEST RESULTS OF THE NOVATEL MILLENNIUM RECEIVER

As a test case, use will be made of EGNOS data recorded at a measurement site at the NLR in the Netherlands with a Novatel Millennium receiver. The data collection on 28 April 2006 started at 0.00 hours and ended at 24.00 hours UTC.

Since the probability density functions are different for the vertical and horizontal case, the discussion is split up into two chapters accordingly.

Integrity of SBAS related to vertical errors

Figure 4 shows time series of the Vertical Position Error (VPE) and the Vertical Protection Level (VPL). From this figure it is clear that during the test the vertical position error was always smaller than the protection level and as a consequence no Misleading Information occurred. At the sample times of about 4.53×10^5 and 4.97×10^5 it can be observed that the absolute value of the position error and the protection level increase approximately simultaneously.

Figure 5 shows a histogram of the Vertical Position Error. This histogram suggests that the VPE is approximately normally distributed. The 95% percentile vertical error is 1.90 m.

Figure 6 shows a histogram of the Vertical Protection Level. The bulk of the protection level data is located around approximately 10 m. Furthermore the occurrence of the protection level data decreases gradually towards larger magnitudes.

Usually one visualizes the integrity risk using the so-called Stanford diagrams. In the figures 7a, 7b and 7c the Stanford diagrams of the APV-I, APV-II and CAT-I aeronautical services are shown. Again from these figures it is clear that no Misleading Information and no Hazardous Misleading Information did occur.

To estimate the MI and HMI probabilities use is made of the probability densities discussed already in this paper.

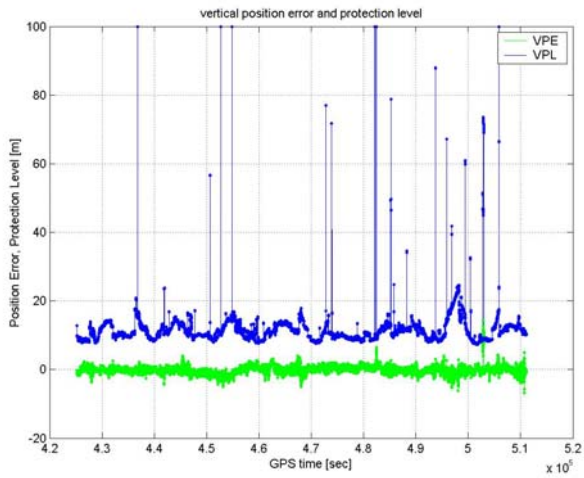


Figure 4: Time series of the vertical position error and the vertical protection level (the maximum vertical scale shown in this figure is 100 m, some VPL values exceed this maximum by far)

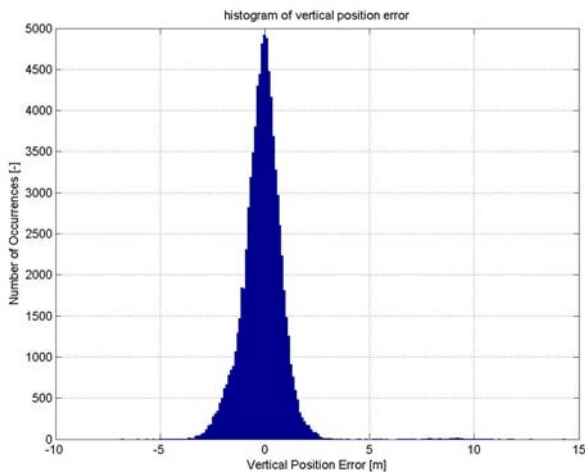


Figure 5: Histogram of the vertical position error.

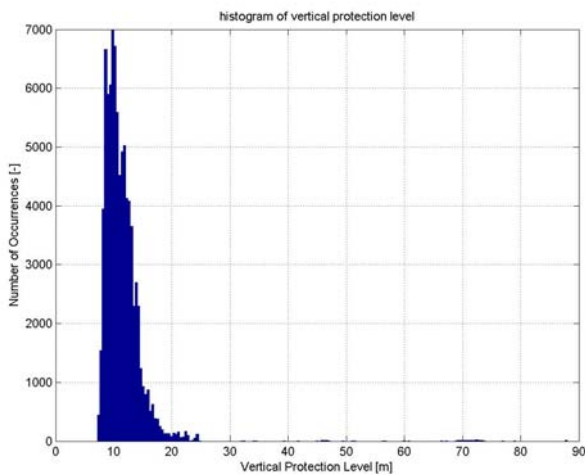


Figure 6: Histogram of the vertical protection level

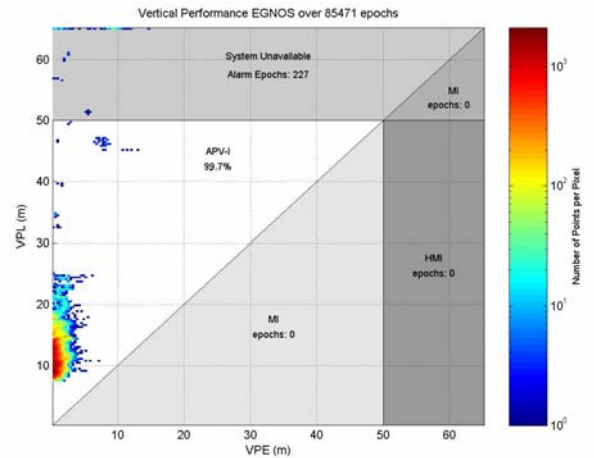


Figure 7a: Stanford diagram for the APV-I service.

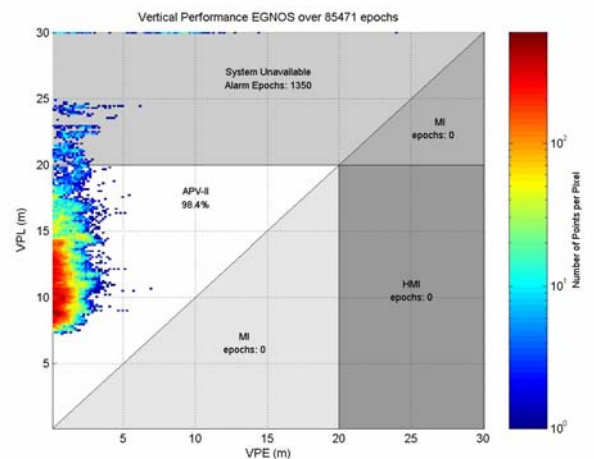


Figure 7b: Stanford diagram for the APV-II service.

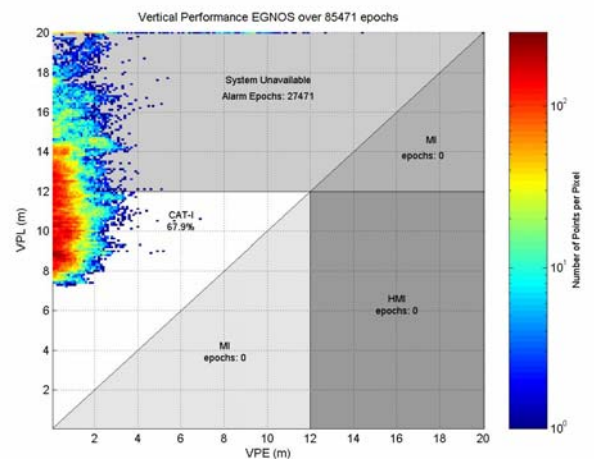


Figure 7c: Stanford diagram for the CAT-I service.

As an example a histogram plot (see figure 8) is made of all measured samples in a slice chosen around the value $VPL_{\text{slice}} = 16.2$ m within the bounds $VPL_{\text{LowerBound}} = 16$ m and $VPL_{\text{UpperBound}} = 16.4$ m. This plot will be used to check if the normal probability distribution is adequate for this particular data set.

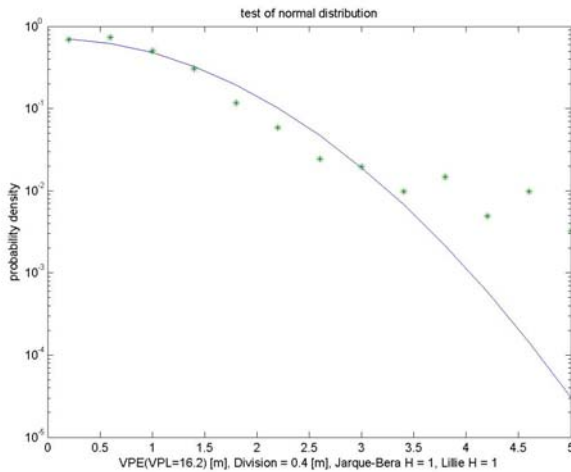


Figure 8: Histogram plot to check if the normal probability distribution is adequate.

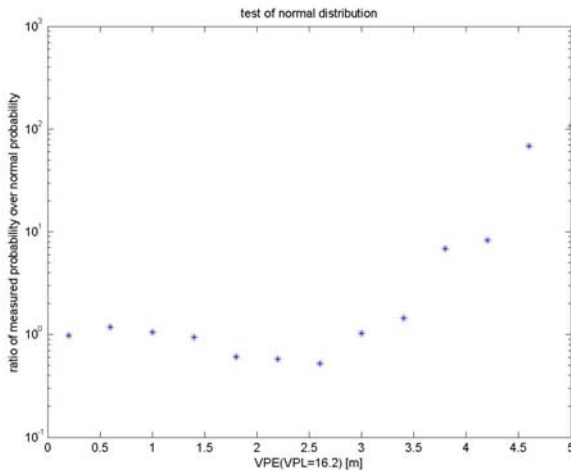


Figure 9: Measured probability divided by normal probability.

The highest value of the vertical position error $VPE = 5$ m shows a probability of around $3 \cdot 10^{-3}$ being 100 times larger than the normal probability of $3 \cdot 10^{-5}$. From this observation it is clear that the measured probability distribution is not normally distributed especially not at the tail. The applied normal probability distribution checks, the Jarque-Bera and the Lilliefors tests, yield the same conclusion. The outlier probabilities can be fitted by a Laplace distribution. To locate the range of outliers to be fitted, a plot of the measured probability divided by the normal probability is made (see figure 9). Applying a

threshold value of 4 it is clear that all four measurement results having a vertical position error larger than 3.5 are outliers. The combination of the normal distribution and the Laplace distribution is shown in figure 10. Figure 10 clearly shows that the outliers satisfy the Laplace probability distribution indeed.

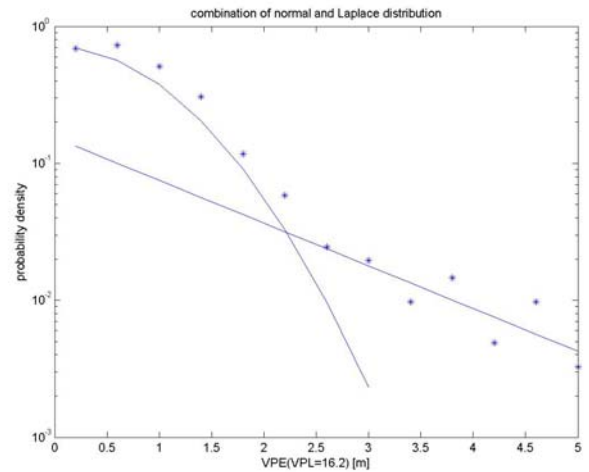


Figure 10: The combination of the normal and Laplace distribution.

The example analysis up to now is based on data occurring within a slice of $VPL_{\text{slice}} = 16.2 \pm 0.2$ m. However, a two dimensional probability density function over the whole range of VPL and VPE is needed. There are three ways to achieve this:

- The two dimensional distribution is the combined set of all individual slices (bins) along the VPL axis. From a theoretical point of view this is the best solution, however, an unpractically large amount of collected data is required then to get a stable result (see the analysis hereafter).
- Perform the statistics on the ratio of the parameters VPE and VPL: the parameter VPE/VPL . However, the assumption made here is that not any bias influence is present in the VPL computation (in this case σ_0 is cancelled in equation 6). In practice however, some bias is always present as will be shown in the analysis hereafter.
- A linear relationship between σ_{VPE} and VPL can be assumed and fitted (equation 6); because of the addition of the two coefficients σ_0 and $const_{VPL}$ in equation 6, which are to be estimated, a better overall fit of the whole two dimensional probability density is the result.

Two dimensional probability density function based on bins along VPL

An analysis is made of probability densities based on the combination of the normal distribution with Laplace distribution within all successive slices defined along the VPL axis. It turns out that only in a part of these slices outliers are found. As a consequence the Laplace distribution coefficients a and b in equation 3 vary within a wide range and are often absent. The plots shown in this chapter only represent the probability distributions at the slices where outliers are found and thus include a Laplace distribution at the tail.

As shown in figure 11, in ten slices (width of the slices is set to 0.2 m) outliers (deviations from the normal distribution) are found. The percentages of outliers ($\alpha \div 100$ in equation 2) in these particular slices are plotted in this figure.

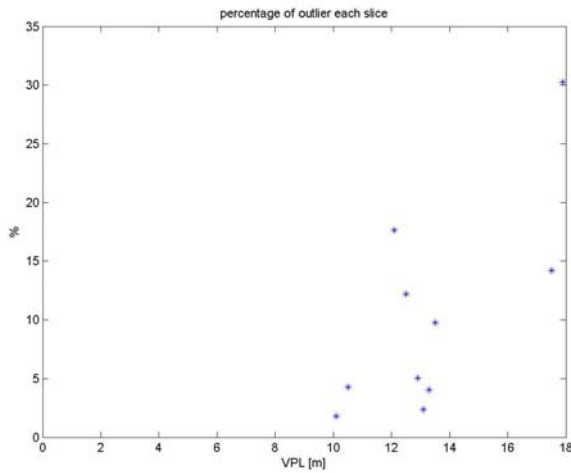


Figure 11: Percentage of outliers in each successive slice.

In figure 12, the extrapolated Laplace probability towards $VPE = 0$ is plotted (coefficient a in equation 3). This figure shows a wide spread in the coefficient a while no clear trend is visible.

Figure 13 shows the slope of the logarithmic Laplace probability distribution (coefficient b in equation 3). This figure shows a wide spread in these slopes while no clear trend is visible.

In order to reduce the spread in the coefficients a and b in equation 3 it seems reasonable to combine all slices such that only one combined Laplace and normal distribution is to be fitted. This can be done by mapping all data into one reference slice using a mapping equation as for example equation 6. This procedure will be discussed in the following.

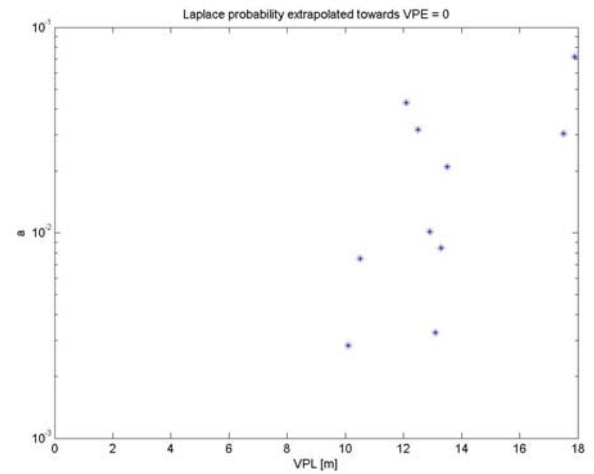


Figure 12: Laplace probability extrapolated towards $VPE = 0$ in each successive slice.

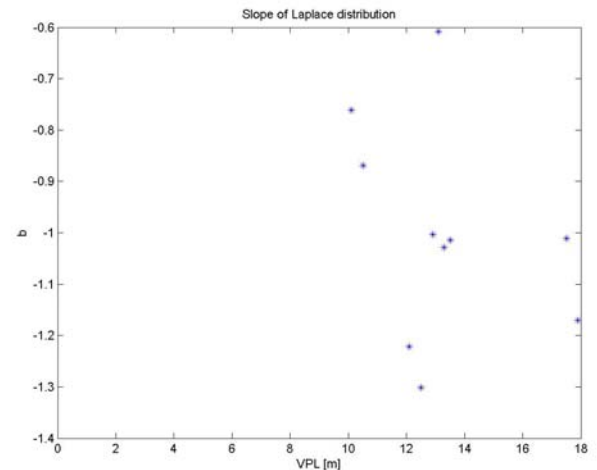


Figure 13: Slope of logarithmic Laplace probability distribution in each successive slice.

Two dimensional distribution with linear dependency of σ_{VPE} to VPL

The standard deviation of all available position error data within each slice along the VPL axis is computed and plotted in figure 14. A straight line (equation 6) has been fitted through these data up to $VPL = 50$ m ($0 < VPL < 50$ is the range of interest for the HMI of the aeronautical services APV-I, APV-II and CAT-I). Figure 14 shows that the intercept σ_0 and the slope $const_{VPL}$ (see equation 6) are both positive, which is in practice almost always the case. Applying this linear relationship leads to a better fit of the two dimensional probability distribution in VPL and VPE direction as compared to the assumption that σ_{VPE} varies in ratio with the VPL. It is now possible to map all VPE data on a reference $VPE_{reference} = 10$ m using equation 6.

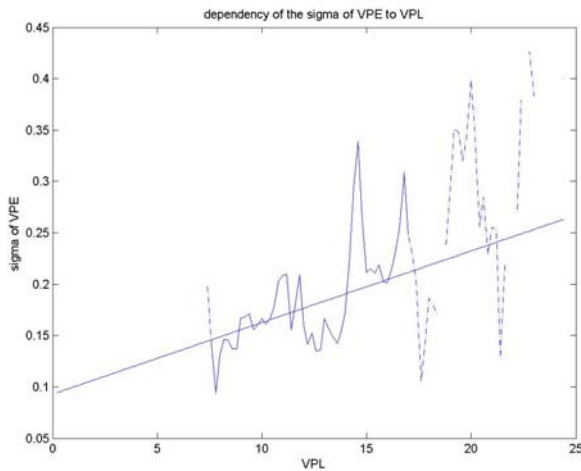


Figure 14: Dependency of the standard deviation of VPE on VPL.

In order to check if the normal probability distribution is adequate for this mapped data set a histogram plot (see figure 15) is made of all measured samples.

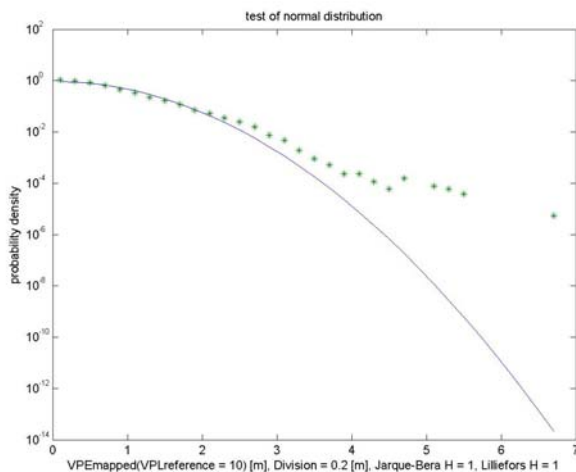


Figure 15: Histogram plot to check if the normal probability distribution is adequate.

The highest value of the vertical position error $VPE_{mapped} = 6.7$ m shows a probability of around 5×10^{-6} being about 2.5×10^8 times larger than the normal probability of 2×10^{-14} . From this observation it is clear that the probability distribution is not normally distributed especially not at the tail. The applied normal probability distribution checks, the Jarque-Bera and the Lilliefors tests, yield the same conclusion.

The combination of the normal distribution and the Laplace distribution is shown in figure 16. This figure clearly shows that the outliers satisfy the Laplace probability density indeed. It can be concluded that a mixture of probability functions is required to describe the measured probability distribution properly

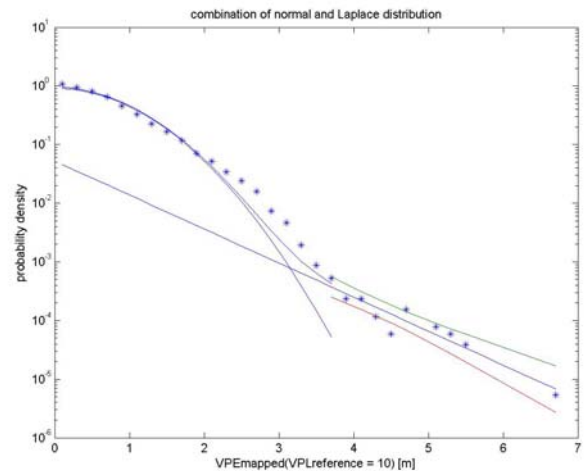


Figure 16: The combination of the normal and Laplace distribution.

However, a two dimensional probability density function over the whole range of VPL and VPE is needed. This can be achieved by mapping the probability density function of figure 16 on the slices defined already along the VPL axis. The integrated probability over each individual slice is determined by the fraction of measured samples within that slice relative to the total number of samples. The MI and HMI risks can now be computed by integrating the two dimensional probability density over the areas of interest. In the figures 17a, 17b and 17c the MI risks and HMI risks for the APV-I, APV-II and CAT-I aeronautical services are plotted. The contours having the values 1, 0.001 and 10^{-10} indicate the probability density relative to the maximum probability density. These figures show that for the APV-I, APV-II and CAT-I services the HMI risks are 1.9×10^{-17} , 7.5×10^{-13} and 7.9×10^{-10} respectively. These risks satisfy the ICAO requirement of 2×10^{-7} per approach (or, approximately, 1.33×10^{-9} per second).

It is good practice to compute the limits for a specified confidence level of the final statistical results. It indicates how much confidence we can put on these results. The problem in computing the confidence interval is the fact that the sampled data are highly correlated in time, while a confidence level can be computed only over uncorrelated data. So we need to de-correlate the data and the question arises what the de-correlation time should be. Since in practice the Misleading Information probability depends almost only on outliers it is sufficient to check the de-correlation time of the appearance of outliers. Figure 18 shows a histogram of outliers (deviations from the normal distribution) as they show up spread over the day of the test. Nearly all outliers appear around 21.³⁰ o'clock. So the outliers show up in one burst and can be considered to be highly correlated over this day. Based on this fact it is decided to treat the outlier data as an uncorrelated data set here, occurring in one burst.

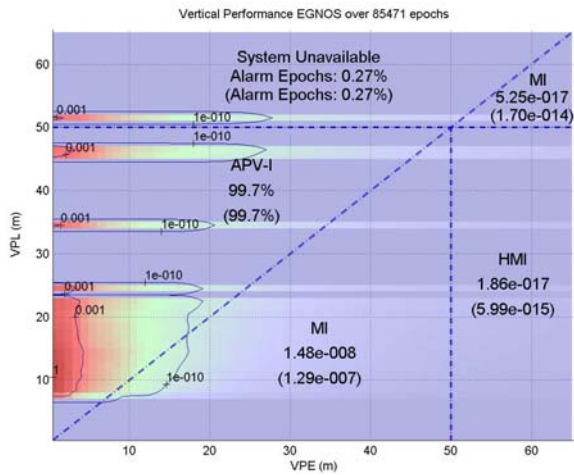


Figure 17a: MI risks and HMI risk for the APV-I service (the values within brackets refer to 95% confidence one sided upper limits).

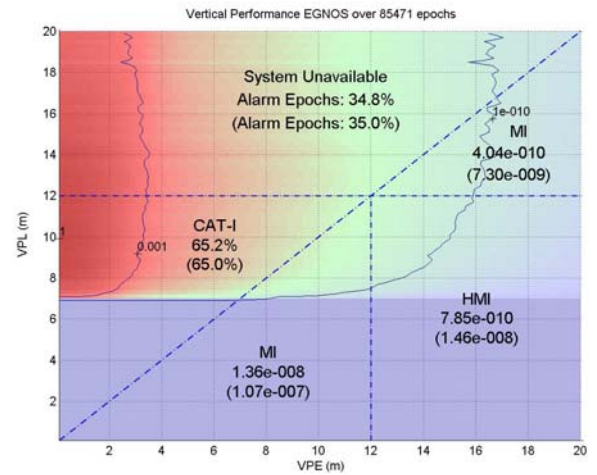


Figure 17c: MI risks and HMI risk for the CAT-I service (the values within brackets refer to 95% confidence one sided upper limits).

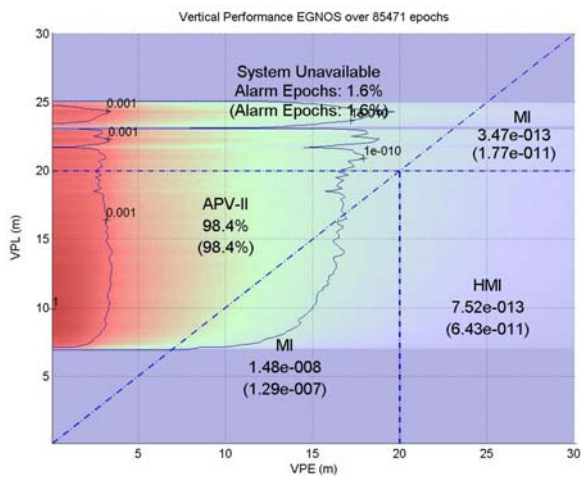


Figure 17b: MI risks and HMI risk for the APV-II service (the values within brackets refer to 95% confidence one sided upper limits).

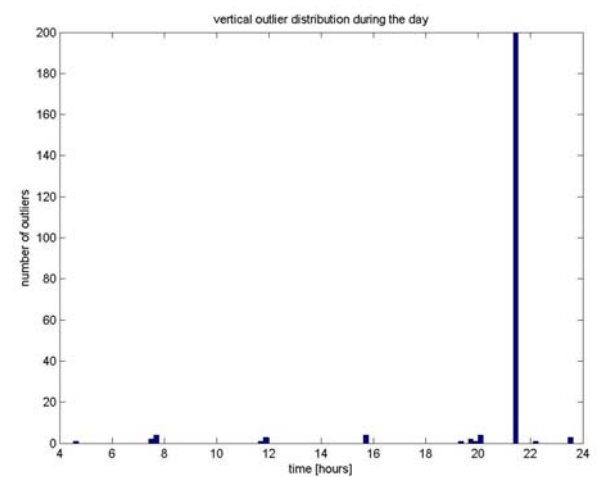


Figure 18: Histogram of outliers spread over the day of the test.

Integrity of SBAS related to horizontal errors

Figure 19 shows time series of the Horizontal Position Error (HPE) and the Horizontal Protection Level (HPL). From this figure it is clear that during this test the horizontal position error was always smaller than the protection level and as a consequence no Misleading Information occurred. At the sample time of about 4.5×10^3 it can be observed that the absolute position error and the protection level increase approximately simultaneously. Figure 20 shows a histogram of the Horizontal Position Error. This histogram suggests that the HPE is approximately Rayleigh distributed indeed. The 95% percentile horizontal error is 1.47 m.

Figure 21 shows a histogram of the Horizontal Protection Level. The bulk of the protection level data is located around approximately 7 m. Furthermore the occurrence of the protection level data decreases gradually towards larger magnitudes. Usually one visualizes the integrity risk using the so-called Stanford diagrams. In figure 22 the Stanford diagram of the APV-II and CAT-I aeronautical services is shown. Again from this figure it is clear that no Misleading Information and no Hazardous Misleading Information did occur. Although the number of observed data points in the MI region is zero in all cases, this does not mean that the true MI and HMI probabilities are zero. To estimate these probabilities use is made of the probability densities discussed already in this paper.

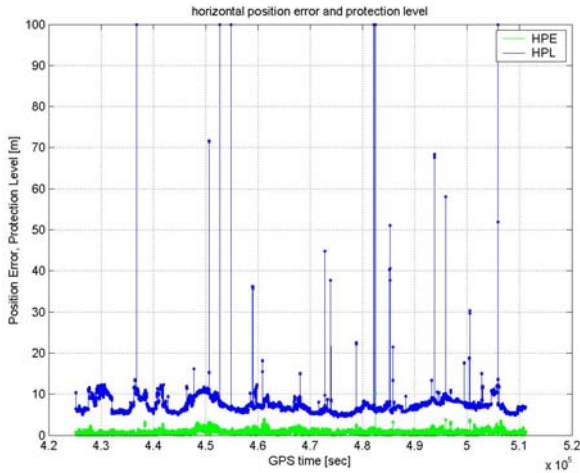


Figure 19: Time series of the horizontal position error and the horizontal protection level (the maximum vertical scale shown in this figure is 100 m, some HPL values exceed this maximum by far)

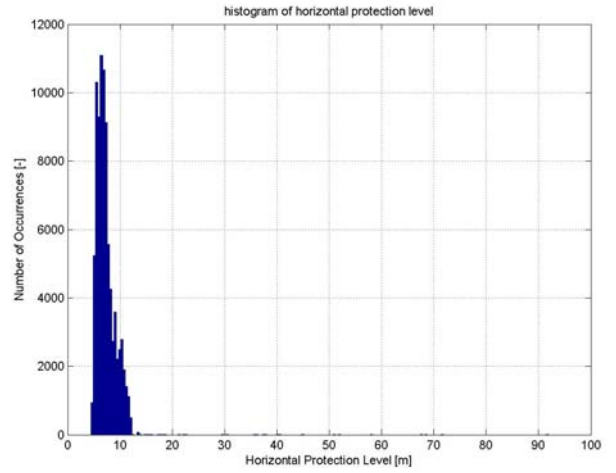


Figure 21: Histogram of the horizontal protection level

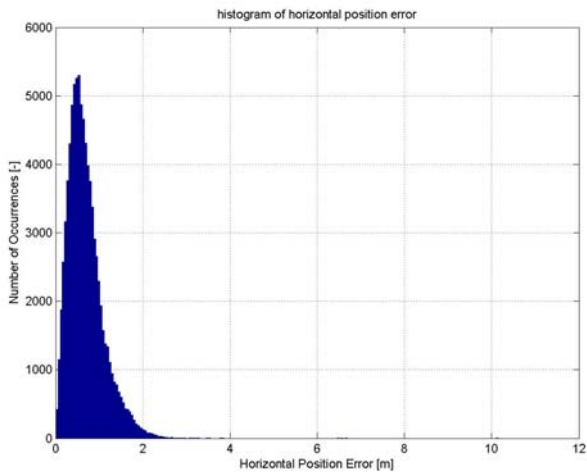


Figure 20: Histogram of the horizontal position error.

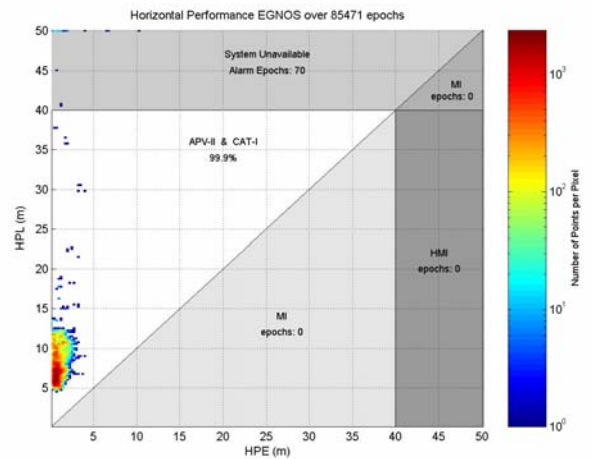


Figure 22: Stanford diagram for the APV-II and CAT-I service.

As an example a histogram plot (see figure 23) is made of all measured samples in a slice chosen around the value $HPL_{\text{slice}} = 6.5 \text{ m}$ within the bounds $HPL_{\text{LowerBound}} = 6.4 \text{ m}$ and $HPL_{\text{UpperBound}} = 6.6 \text{ m}$. This plot will be used to check if the Rayleigh probability distribution is adequate for this particular data set

The highest value of the vertical position error $HPE = 3.5 \text{ m}$ shows a probability of around $3 \cdot 10^{-4}$ being more than 10^5 times larger than the Rayleigh probability of $7 \cdot 10^{-10}$. From this observation it is clear the measured probability distribution is not Rayleigh distributed especially not at the tail. The outlier probability distribution can be fitted by a Laplace distribution.

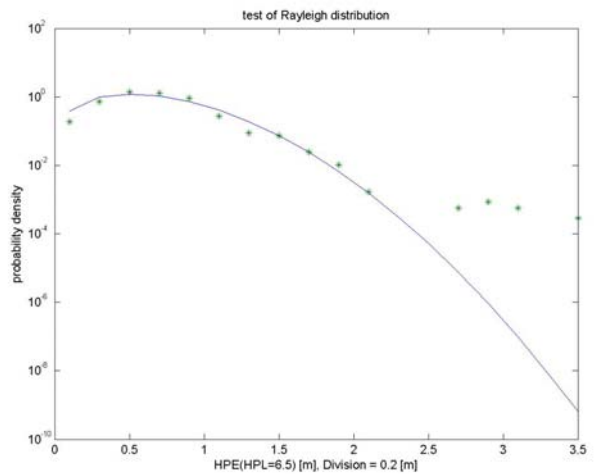


Figure 23: Histogram plot to check if the Rayleigh probability distribution is adequate.

Figure 24 clearly shows that the outliers satisfy the Laplace probability distribution indeed.

The example analysis up to now is based on data occurring within a slice of $HPL_{slice} = 6.5 \pm 0.1$ m. However, a two dimensional probability density function over the whole range of HPL and HPE is needed. Therefore similarly to the vertical case we choose a linear relationship between σ_{HPE} and HPL

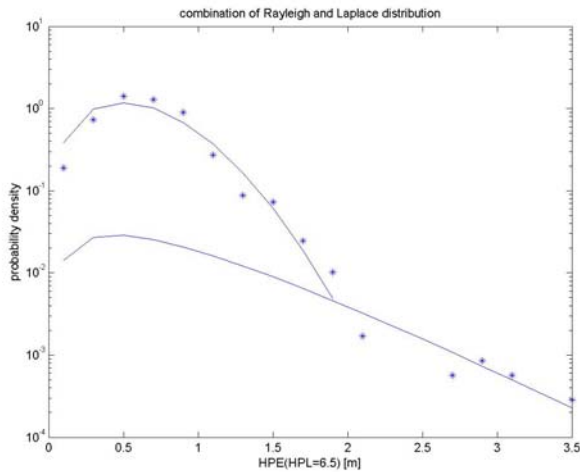


Figure 24: The combination of the Rayleigh and Laplace distribution.

The Rayleigh standard deviation of the position error of each slice along the HPL axis is computed and fitted with a straight line (equation 6) up to $HPL = 40$ m ($0 < HPL < 40$ is the range of interest for the HMI of the aeronautical services APV-II and CAT-I). The result is shown in figure 25.

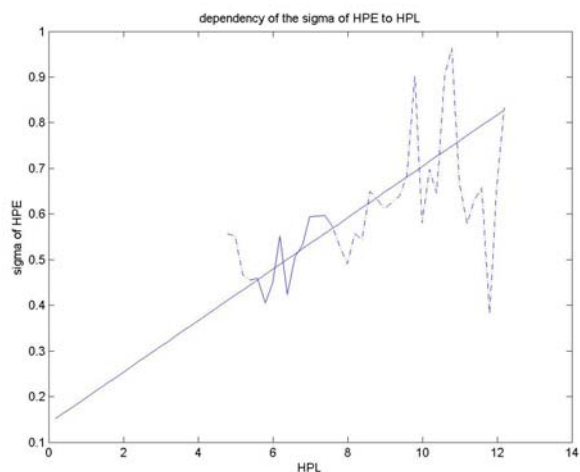


Figure 25: Dependency of the Rayleigh standard deviation of HPE on HPL.

Figure 25 shows that the intercept σ_0 and the slope $const_{HPL}$ (see equation 6) are both positive, which is in practice almost always the case. Applying this linear

relationship leads to a better fit of the two dimensional probability distribution in HPL and HPE direction as compared to the assumption that σ_{HPE} varies in ratio with the HPL. It is now possible to map all HPE data on a reference $HPE_{reference} = 10$ m using equation 6.

In order to check if the Rayleigh probability distribution is adequate for this mapped data set a histogram plot (see figure 26) is made of all measured samples.

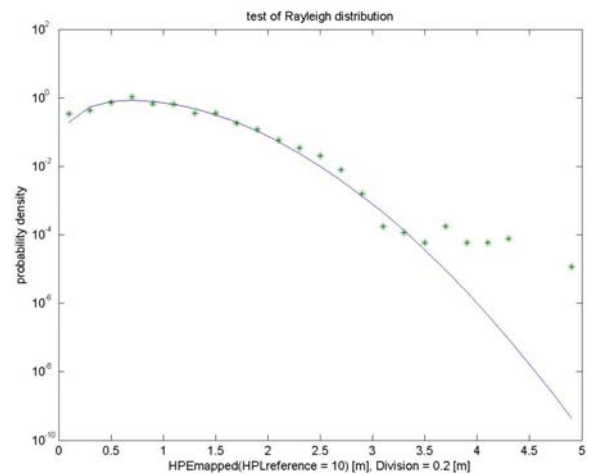


Figure 26: Histogram plot to check if the Rayleigh probability distribution is adequate.

The highest value of the horizontal position error $HPE_{mapped} = 4.9$ m shows a probability of around 10^{-5} being about 2×10^4 times larger than the Rayleigh probability of 5×10^{-10} . From this observation it is clear that the measured probability distribution is not Rayleigh distributed especially not at the tail. The outlier probability distribution can be fitted by a Laplace distribution.

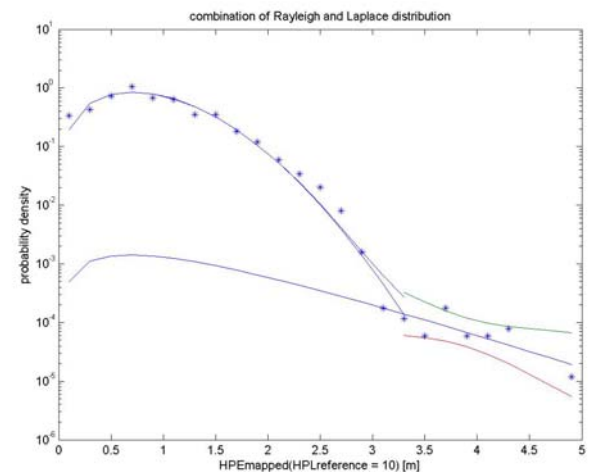


Figure 27: The combination of the Rayleigh and Laplace distribution.

Figure 27 clearly shows that the outliers satisfy the Laplace probability density indeed.

However, a two dimensional probability density function over the whole range of HPL and HPE is needed. This can be achieved by mapping the probability density function of figure 27 on the slices defined already along the HPL axis. The integrated probability over each individual slice is determined by the fraction of measured samples within that slice. The MI and HMI risks can now be computed by integrating the two dimensional probability density over the areas of interest. In the figure 28 the MI risks and HMI risk for the APV-II and CAT-I services are plotted. The contours having the values 1, 0.001 and 10^{-10} indicate the probability density relative to the maximum probability density. The HMI risk is 7.9×10^{-15} . This risk satisfies the ICAO requirement of 2×10^{-7} per approach (or, approximately 1.33×10^{-9} per second).

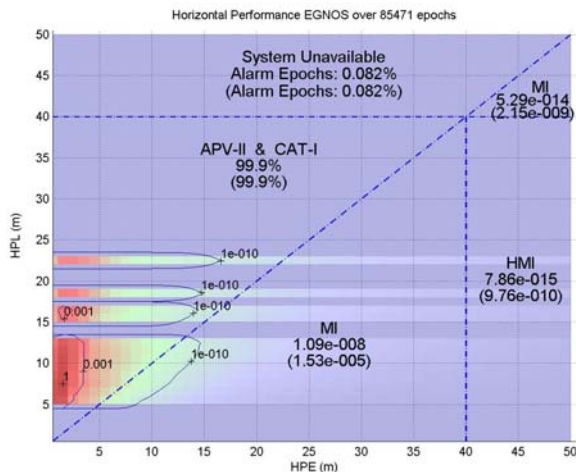


Figure 28: MI risks and HMI risk for the APV-II and CAT-I services (the values within brackets refer to 95% confidence one sided upper limits).

Overview of the test results

From the presented analysis it can be concluded that EGNOS satisfy the requirements of the APV-I, APV-II and CAT-I services as far as the Hazardous Misleading Information is concerned.

The probabilities without outliers were computed by integrating probability distributions after subtraction of the Laplace distributions. The probabilities without outliers turn out to be rather optimistic indeed (e.g the HMI risk for CAT-I is 9×10^{-41}). So the conclusion is justified that the analysis of outliers is absolutely necessary to obtain realistic results. From this it follows that the duration of the data set must be such that outliers can be identified.

The probability of Misleading Information turns out to be 1.5×10^{-8} . This means that from a theoretical point of view some Alarm Limit value may exist resulting into an HMI

probability exceeding the value of 1.33×10^{-9} per second (this is approximately the ICAO requirement). So, as a matter of fact, there is a relatively small margin in the conclusion that the HMI requirement of the APV-I, APV-II and CAT-I services is satisfied.

Furthermore, the 95% confidence upper limit of the HMI probability for the CAT-I aeronautical service is 1.46×10^{-8} being 11.0 times as large as the required 1.33×10^{-9} . From this we may conclude that, from a statistical perspective, we should extend this test campaign to 121 days ($121 = 11.0^2$) instead of the actual test of one day. Once all these 121 test days do show, from a statistical perspective, a similar behaviour, the required integrity will then be proven within a confidence level of 95%.

CONCLUSIONS

A test method has been developed to analyse receiver output data gathered during a test campaign of limited duration for EGNOS and for the future Galileo system. The method is designed to handle outliers possibly present in the data set. It turns out that the analysis of outliers is absolutely necessary to obtain useful results. From the test case presented in this paper, it can be concluded that the estimation of the integrity, on the basis of a limited number of test campaign data, accurately is possible indeed. The results show that the integrity satisfied the ICAO requirement for the APV-I, APV-II and CAT-I aeronautical services during this test.

REFERENCES

- [1] RTCA/DO-229C, Minimum Operational Performance Standards for Global Positioning System/Wide Area Augmentation System Airborne Equipment. 2001.
- [2] M. Tossaint, J. Samson, F. Toran, J. Ventura-Traveset, J. Sanz, M. Hernandez-Pajares, J.M. Juan. The Stanford – ESA Integrity Diagram : Focusing on SBAS Integrity. ION 2006.
- [3] A. Pacipico, M. Vultaggio. EGNOS: First Results of the European SBAS System. European Navigation Conference 2006, Manchester UK.